Supporting Information

The Polymorphism of 2-benzoyl-*N,N*-diethylbenzamide

Lygia S. de Moraes [1,*], Jie Liu [1], Elumalai Gopi [1], Ryusei Oketani [1], Alan R. Kennedy [2] and Yves H. Geerts [1,3,*]

[1] Laboratoire de Chimie des Polymères, Faculté des Sciences, Université Libre de Bruxelles (ULB), Boulevard du Triomphe, CP 206/01, 1050 Bruxelles, Belgium; jie.liu@ulb.be (J.L.); gopi.elumalai@ulb.be (E.G.); oketani@chem.es.osaka-u.ac.jp (R.O.)
[2] WestCHEM, Department of Pure & Applied Chemistry, University of Strathclyde, Glasgow G1 1XL, Scotland; a.r.kennedy@strath.ac.uk
[3] International Solvay Institutes of Physics and Chemistry, ULB - Campus Plaine - CP 231 Boulevard du Triomphe, 1050 Brussels, Belgium
* Correspondence: lygia_moraes@hotmail.com (L.S.M.); yves.geerts@ulb.be (Y.H.G.)

Table of Contents

1. Synthesis

All reactants and solvents were obtained from Sigma Aldrich and were used without further purification. Synthesis of 2-benzoyl-N,N-diethylbenzamide (BDB, **Error! Reference source not found.**) was carried following the synthesis route described by Wei *et al.* (2015) [1]. A solution of diethylamine (1.372 mL, 13.26 mmol) and 2-benzoylbenzoic acid (3 g, 13.26 mmol) in DCM (125 ml) was prepared and the mixture was stirred for five minutes. N-ethyl-N-isopropylpropan-2-amine (2.72 mL, 15.59 mmol) and N,N-dimethylpyridin-4-amine (0.162 g, 1.326 mmol) were added successively. The reaction mixture was stirred for 15 h at room temperature. After the completion of the reaction as shown by TLC, water (30 mL) was used to dilute the reaction mixture. The organic layer was extracted with DCM (20 mL × 3). The combined organic layer was washed with saturated brine (30 mL), dried over anhydrous magnesium sulphate and concentrated under vacuum. The crude product was purified by flash chromatography (ethyl acetate/petroleum ether = 1:1) to give 2-benzoyl-N,N-diethylbenzamide ($C_8H_{19}NO_2$, mw = 281.35 g/mol, m = 2.89 g, 77 % yield).

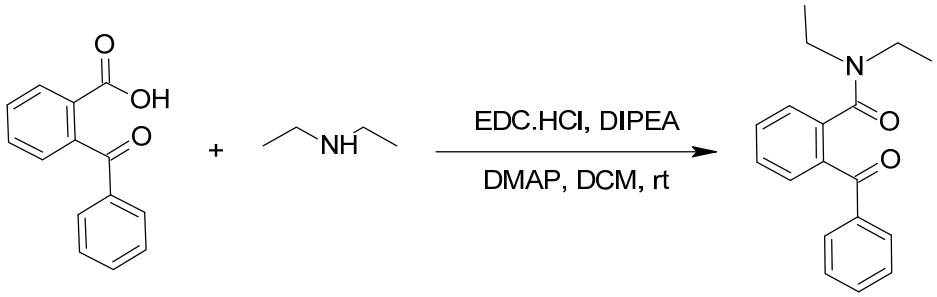

Scheme S1. Synthesis route of 2-benzoyl-N,N-diethylbenzamide (BDB).

2. Nuclear Magnetic Resonance (NMR)

^{1}H and ^{13}C NMR spectra of 2-benzoyl-N,N-diethylbenzamide were collected on a Jeol 400 MHz spectrometer from a deuterated chloroform solution. Chemical shifts (in ppm), multiplicity (m = multiplet and q = quintet) and the coupling constant (J, in Hz) are shown below and the spectra are shown in Figure S1 and Figure S2, for ^{1}H and ^{13}C NMR, respectively.

^{1}H NMR (400 MHz, $CDCl_3$) δ: 7.80-7.76 (m, 2H), 7.54-7.47 (m, 3H), 7.44-7.36 (m, 4H), 3.40 (q, *J* = 6.8 Hz, 2H), 3.23 (q, *J* = 6.8 Hz, 2H), 1.06 (m, 6H).

^{13}C NMR (100 MHz, $CDCl_3$) δ: 196.7, 170.0, 138.4, 137.3, 137.0, 133.1, 130.8, 130.3, 129.9, 128.3, 128.2, 126.8, 77.5, 77.2, 76.9, 43.3, 38.9, 13.8, 12.2.

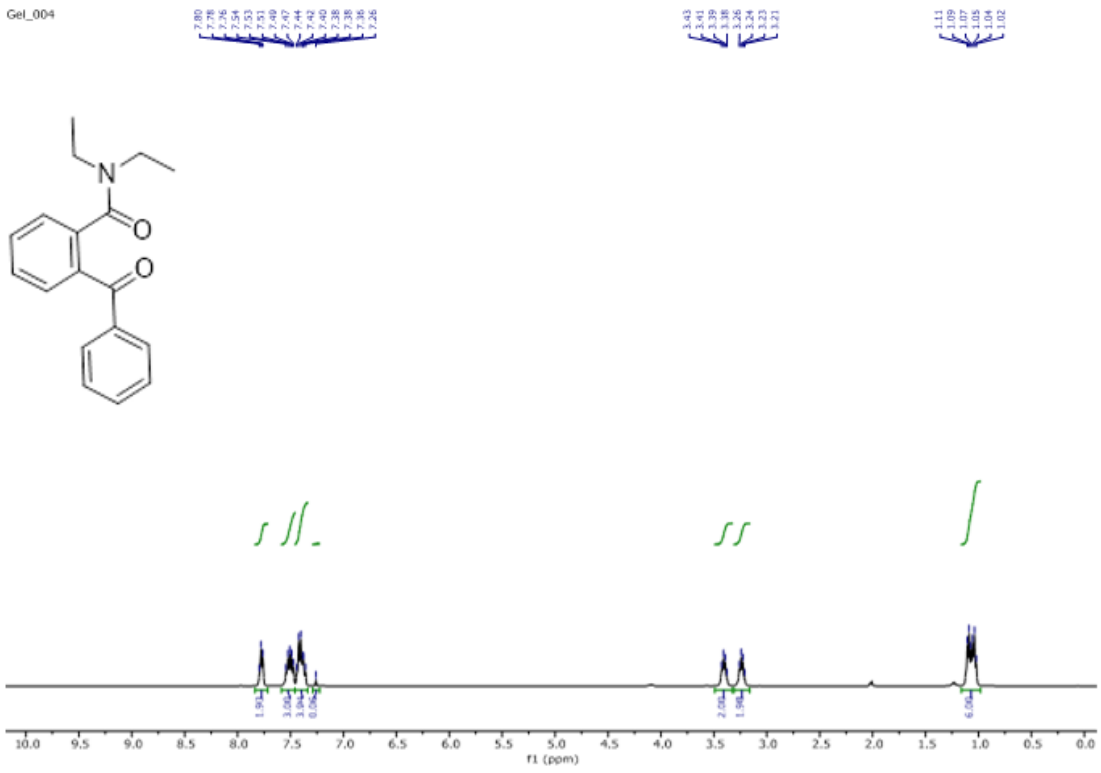

Figure S1. ^{1}H NMR spectra of 2-benzoyl-N,N-diethylbenzamide in $CDCl_3$ solution.

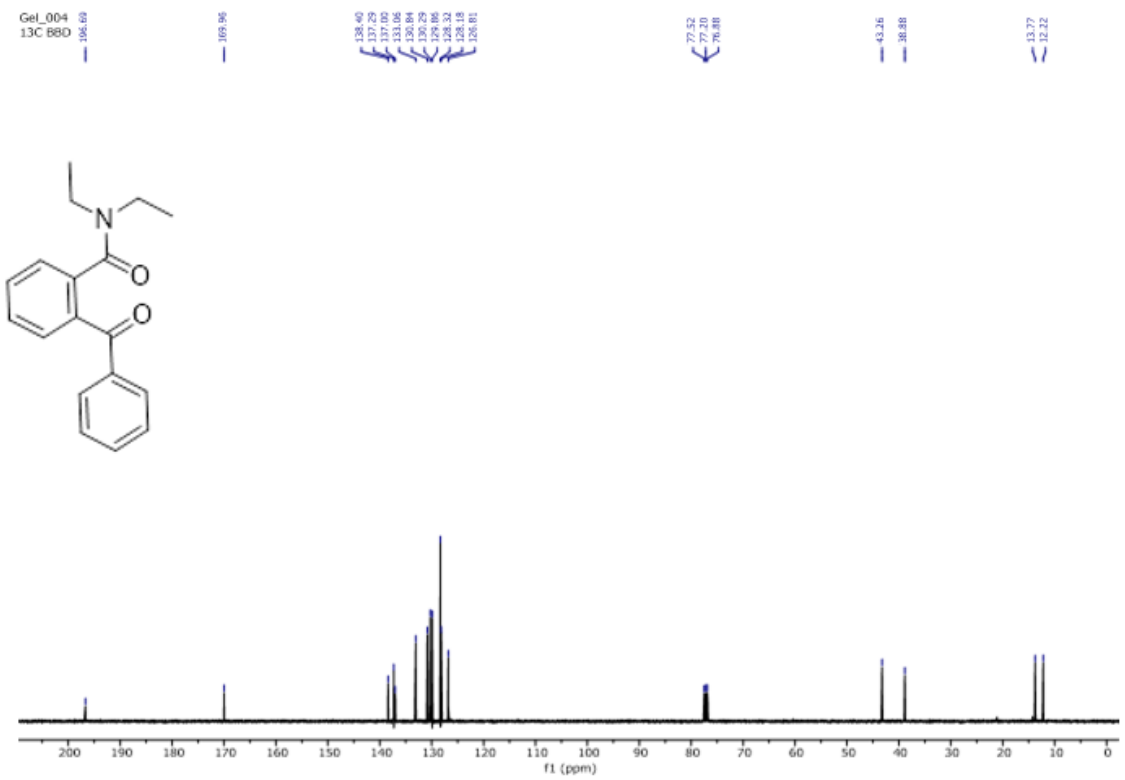

Figure S2. ^{13}C NMR spectra of 2-benzoyl-N,N-diethylbenzamide in $CDCl_3$ solution.

3. X-Ray Powder Diffraction (XRPD)

Experimental and calculated x-ray powder diffraction patterns can be observed in Figure S3 for the confirmation of the phase of the bulk powder after synthesis and recrystallisation using dichloromethane and hexane:chloroform. **Figure S3.** Powder diffraction patterns for the calculated form I (in black. Refcode = BERDOS), calculated form II (in red), calculated form III (in blue), synthesis product batch (in cyan)Variations in the unit cell parameters when compared with the crystal structure obtained with SXD are consequence of the temperature difference between measurements (SXD measured at 150 K and XRPD measured at RT).

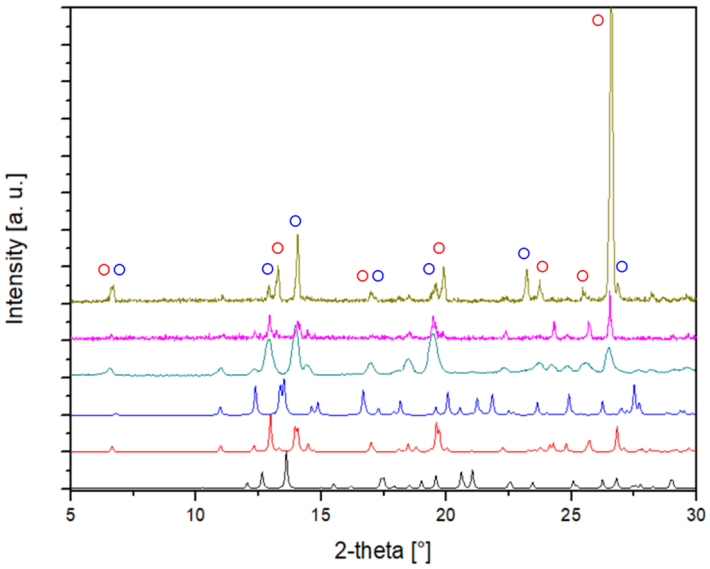

Figure S3. Powder diffraction patterns for the calculated form I (in black. Refcode = BERDOS), calculated form II (in red), calculated form III (in blue), synthesis product batch (in cyan), BDB recrystallised by hexane:chloroform (in pink) and recrystallised by dichloromethane (in beige).

4. List of structures and torsion angles used in the database survey

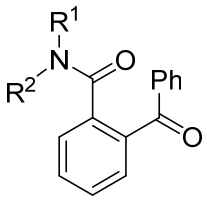

BERDUY: R^1 = Et, R^2 = CH_2Ph
BERFAG: R^1 = CH_2Ph, R^2 = CH_2Ph
NOSYEZ: R^1R^2 = CH_2CH_2-O-CH_2CH_2
OBEXOI and **OBEXOI01:** R^1 = R^2 = Me
OBEXUO: R^1 = Me, R^2 = Ph

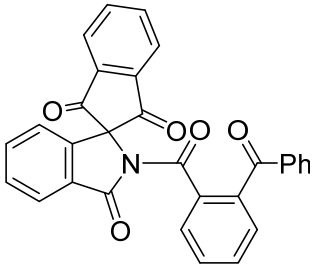

SONFUZ

Figure S4. Molecular structure of the compounds mentioned in the database survey.

Table S1. Label and torsion angles values used in the database survey for the nine structures analysed.

Pair		Atom Label	Torsion Angle [°]			
			BDB-I	BDB-II	BDB-III	BERDUY
1	a	C13-C4-C10-O2	21.59	-26.14	-26.43	-20.47
	b	C6-C4-C10-O2	-157.20	149.92	149.80	155.16
2	a	C13-C4-C10-C3	-154.94	157.30	158.07	160.05
	b	C6-C4-C10-C3	26.27	-26.64	-25.70	-24.33
3	a	C4-C10-C3-C5	48.34	-50.33	-51.24	-34.91
	b	C4-C10-C3-C2	-134.75	130.83	129.88	150.32
4	a	O2-C10-C3-C5	-128.26	133.07	133.20	145.60
	b	O2-C10-C3-C2	48.65	-45.78	-45.68	-29.17
5	a	C10_C3_C2_C7	-177.00	-177.30	-178.46	177.76
	b	C10_C3_C2_C1	12.86	-6.31	-6.92	-6.10
6	a	C3-C2-C1-O1	53.64	-51.83	-51.61	-82.49
	b	O1-C1-C2-C7	-116.45	118.97	119.83	93.71

7	a	C3-C2-C1-N1	-131.64	130.86	130.10	101.93
	b	N1-C1-C2-C7	58.26	-58.34	-58.47	-81.88
Pair		Torsion Angle [°]				
		BERFAG	NOSYEZ	OBEXOI	OBEXUO	SONFUZ
1	a	32.02	14.87	-18.89	28.53	-39.12
	b	-146.60	-161.28	160.17	-149.35	138.99
2	a	-147.25	-165.33	160.17	-152.67	136.53
	b	34.14	18.52	-20.77	29.45	-45.37
3	a	43.97	53.80	-43.85	31.97	-27.27
	b	-138.69	-129.83	142.78	-152.44	160.63
4	a	-135.30	-126.40	135.23	-149.26	148.37
	b	42.04	49.97	-38.14	26.34	-23.72
5	a	-178.74	-176.08	174.34	-177.08	170.35
	b	8.63	12.52	-13.58	13.36	-6.65
6	a	60.16	65.80	-65.98	63.37	-55.93
	b	-112.27	-105.42	106.15	-106.39	121.17
7	a	-121.23	-116.64	118.42	-121.38	118.92
	b	66.35	72.14	-69.45	68.86	-63.98

5. Hirshfeld Surfaces

The software *CrystalExplorer*17 calculate Hirshfeld surfaces based on the contact distance between molecules (d_{norm}) [2-4]. This distance is represented on a Hirshfeld surface by the colour of spots or regions: Red spots represent shorter distances between molecules in comparison with van der Walls distances. White regions show lengths similar to VdW distances while blue regions show distances longer than the VdW distances. The value of d_{norm} can be calculated by Equation S1:

$$d_{norm} = \frac{(d_i - r_i^{vdw})}{r_i^{vdw}} + \frac{(d_e - r_e^{vdw})}{r_e^{vdw}}$$

Equation S1

where, the distances between a point on the surface and the closest nucleus to the surface are represented by d_e for an external nucleus and d_i for an internal nucleus, and r_i^{vdw} and r_e^{vdw} are the internal and external van der Waals radii of the atoms, respectively. From the calculated Hirshfeld Surfaces it is also possible to calculate the 2D fingerprint plots. [2,6] The fingerprint plots are based on how frequent is the occurrence of a combination of d_e and d_i on the surface of a molecule and the colour of the plots shows the contribution between intermolecular contacts where blue, green and red points represents low, medium and high contribution, respectively.

Hirshfeld surfaces (-0.1 Å < d_{norm} < 1.5 Å), fingerprint plots and voids for each form of 2-benzoyl-N,N-diethylbenzamide can be observed in Figure S5 (form I), Figure S6 (form II), Figure S7 (form III). Details of calculated values of Hirshfeld Surface or void volume, area, globularity and asphericity can be found in Table S2.

Table S2. Calculated values of volume, area, globularity and asphericity for the Hirshfeld Surfaces and voids of the three forms of 2-benzoyl-N,N-diethylbenzamide.

	Form	Label	Volume (Å^3)	Area (Å^2)	Globularity	Asphericity
Hirshfeld Surface	form I	1	371.67	337.11	0.742	0.145
	form II	2	376.45	309.34	0.815	0.056
	form III	3	368.49	306.12	0.812	0.057
Void	form I	1	154.36	536.96	0.259	0.082

	form II	2	378.14	1111.43	0.228	0.360
	form III	3	320.17	971.08	0.233	0.398

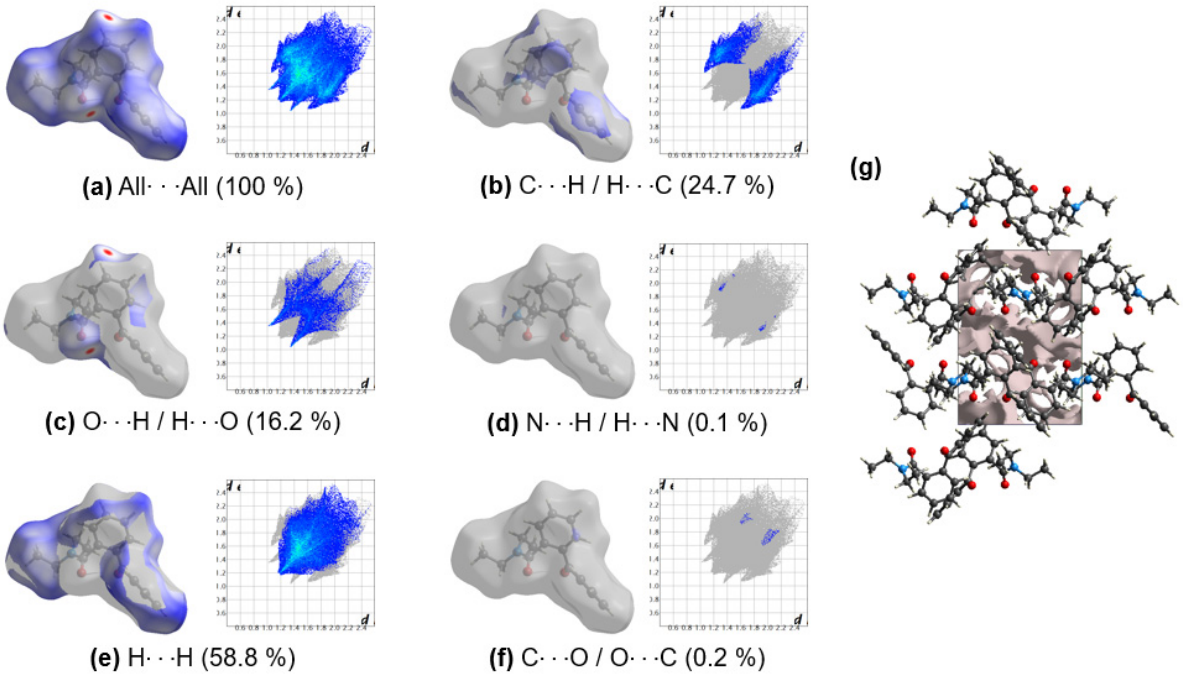

Figure S5. Hirshfeld surfaces and fingerprint plots showing all interactions (a), only C···H/H···C interactions (b), only O···H/H···O interactions (c), only N···H/H···N interactions (d), only H···H interactions (e), only C···O/O···C interactions (f) and voids in the unit cell (g) of the sample form I (refcode: BERDOS).

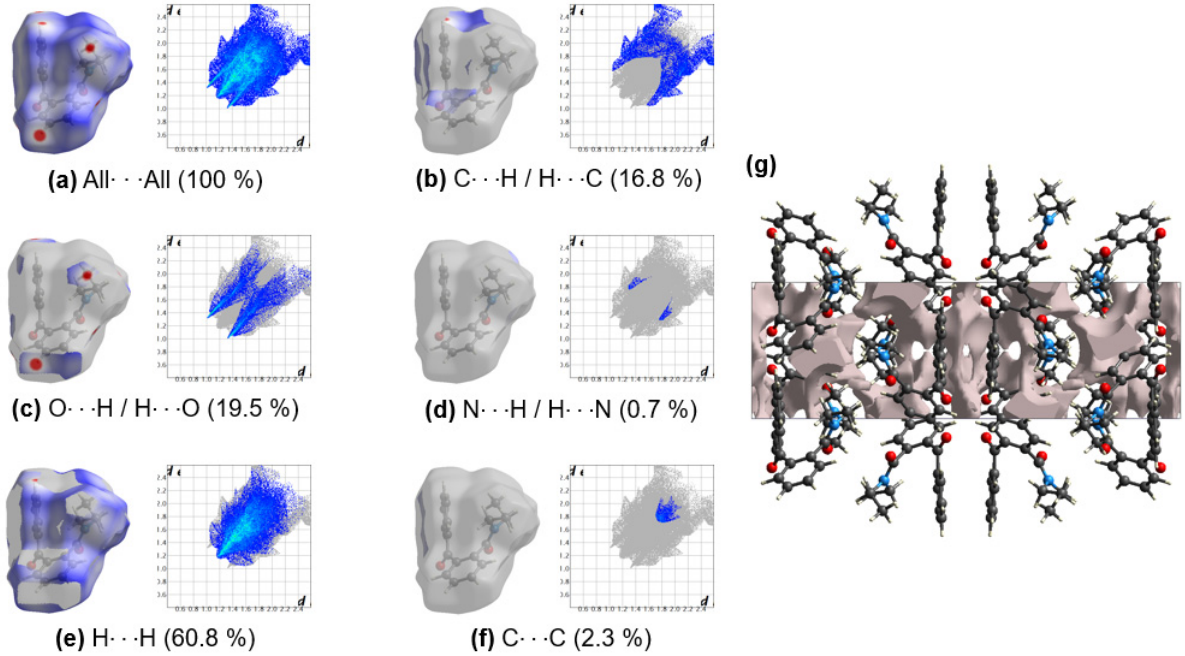

Figure S6. Hirshfeld surfaces and fingerprint plots showing all interactions (a), only C···H/H···C interactions (b), only O···H/H···O interactions (c), only N···H/H···N interactions (d), only H···H interactions (e), only C···C interactions (f) and voids in the unit cell (g) for the sample form II.

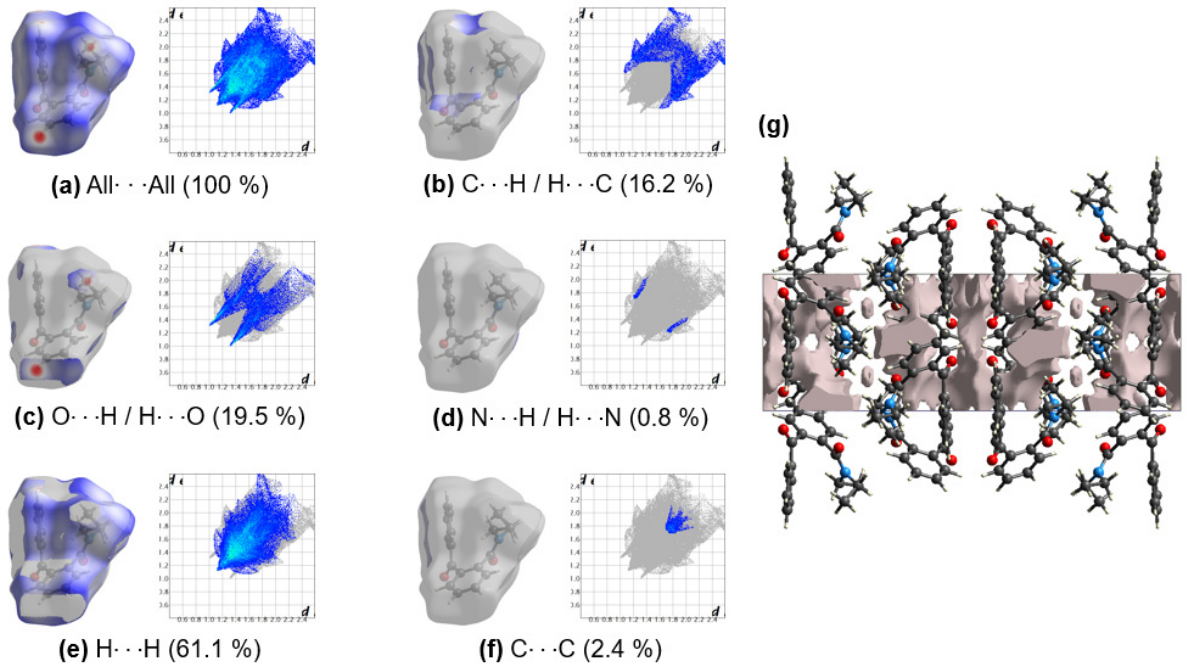

Figure S7. Hirshfeld surfaces and fingerprint plots showing all interactions (a), only C···H/H···C interactions (b), only O···H/H···O interactions (c), only N···H/H···N interactions (d), only H···H interactions (e), only C···C interactions (f) and voids in the unit cell (g) for the sample form III.

6. Thermal characterisation (DSC and TGA)

TGA and DSC was performed for the title compound as mentioned in the article. A summary of the results can be observed in Table S3. Figure S8 shows heating profile of BDB using TGA and Figure S9 shows the two runs of heating and cooling using DSC.

Table S3. TGA and DSC parameters and results for the sample BDB.

	Mass (mg)	Temperature Range (°C)	Run	Temperature Profile	Speed (°C /min)	Temperature (°C)			Enthalpy (kJ/mol)	
						$T_{d/m}$	T_g	T_{crack}	ΔH_m	ΔH_{crack}
TGA	7.789	30 to 500	1st	Heating	10.00	245.1	-	-	-	-
DSC	4.224	-50 to 90	1st	Heating	0.50	51.2	-	-	24.32	-
				Cooling	0.75	-	-	-42.8	-	-0.05
			2nd	Heating		53.9	-20.8	-	0.55	-
				Cooling	1.00	-	-	-42.9	-	-0.01

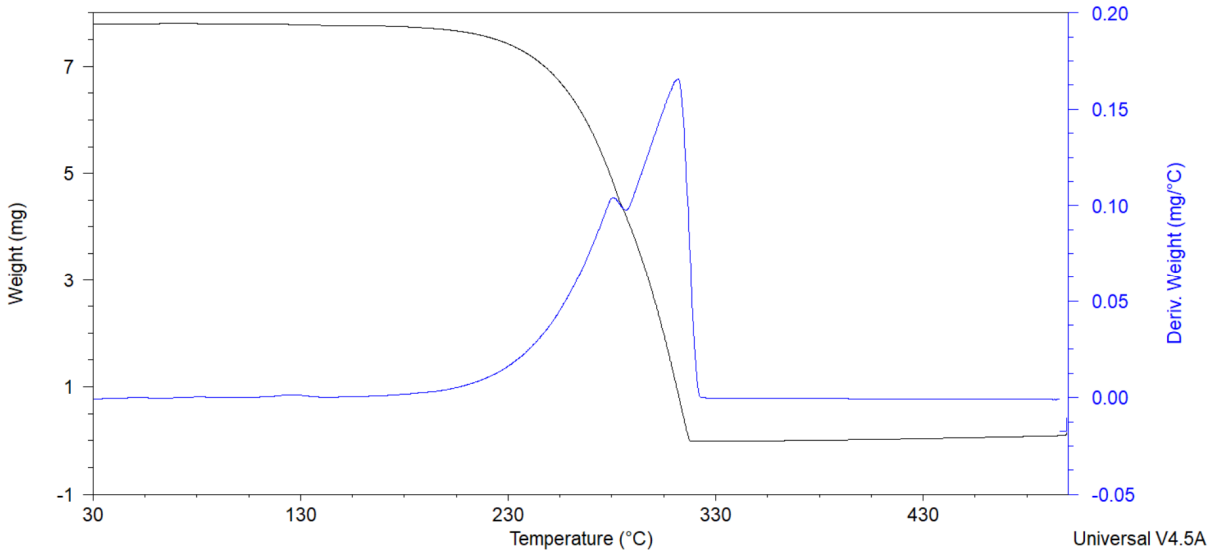

Figure S8. TGA curve heating the sample form II from 30 °C to 500 °C with step of 10 °C/min

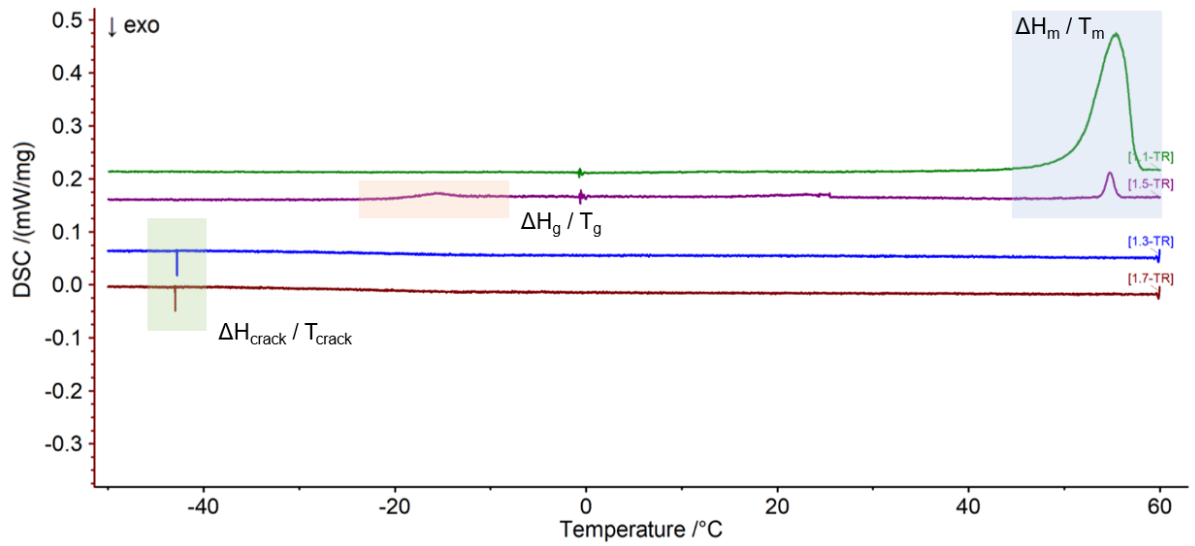

Figure S9. DSC heating and cooling curves for the sample form II. Curve in green represents the 1st heating (0.50 °C/min), in blue the 1st cooling (0.75 °C/min), in purple the 2nd heating and in brown the 2nd cooling.

7. Variable Temperature X-Ray Powder Diffraction (VT-XRPD)

Experiment 1

Two experiments using VT-XRPD were performed using form II. In experiment 1, the sample was heated from room temperature up to 60 °C where the compound was completely molten. The diffraction patterns can be observed in Figure S10, while the refined unit cell parameters are detailed in Table S4. Once the system was cooled, the compound crystallised as form II with preferred orientation in the c direction, as observed in Figure S11.

Table S4. Variation of the unit cell parameters according to the temperature for the sample **BDB**.

T (°C)	*T* (K)	*a* (σ_a) / Å	*b* (σ_b) / Å	*c* (σ_c) / Å	β (σ_β) / °	*V* (σ_V) / Å	R_p (%)	R_{wp} (%)	Space Group
25	293	13.730 (5)	8.381 (3)	26.878 (8)	90.57 (2)	3093 (2)	12.37	16.45	*I* 2/a
30	303	13.713 (5)	8.389 (3)	26.867 (7)	90.57 (2)	3091 (2)	12.38	16.38	
40	313	13.691 (4)	8.391 (3)	26.807 (8)	90.54 (2)	3080 (2)	9.97	12.45	
50	323	13.689 (4)	8.358 (3)	26.76 (8)	90.42 (2)	3061 (2)	10.73	13.68	

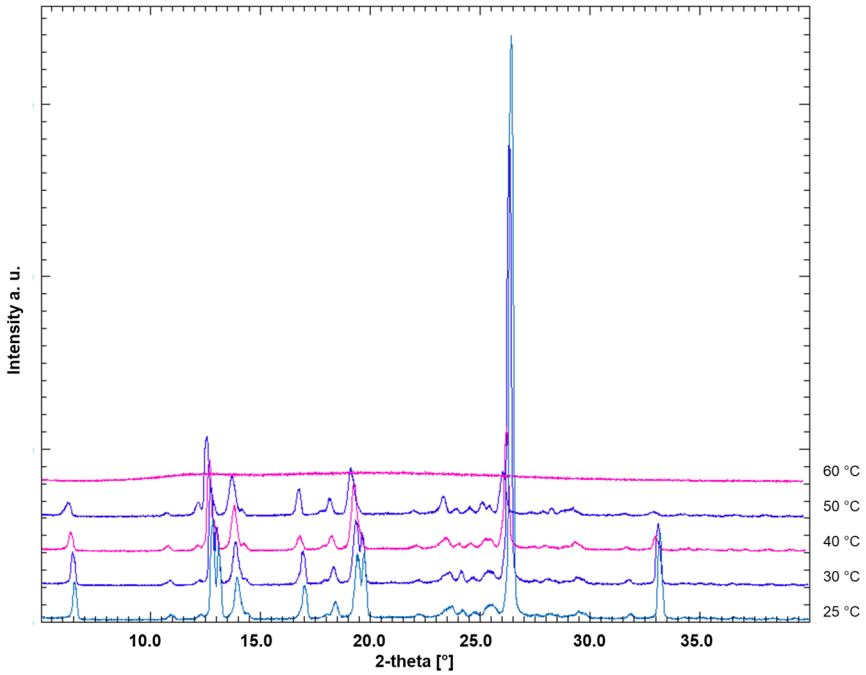

Figure S10. Diffractograms for variable temperature x-ray powder diffraction experiments in 5 different temperature points (T range between 25 °C and 60 °C).

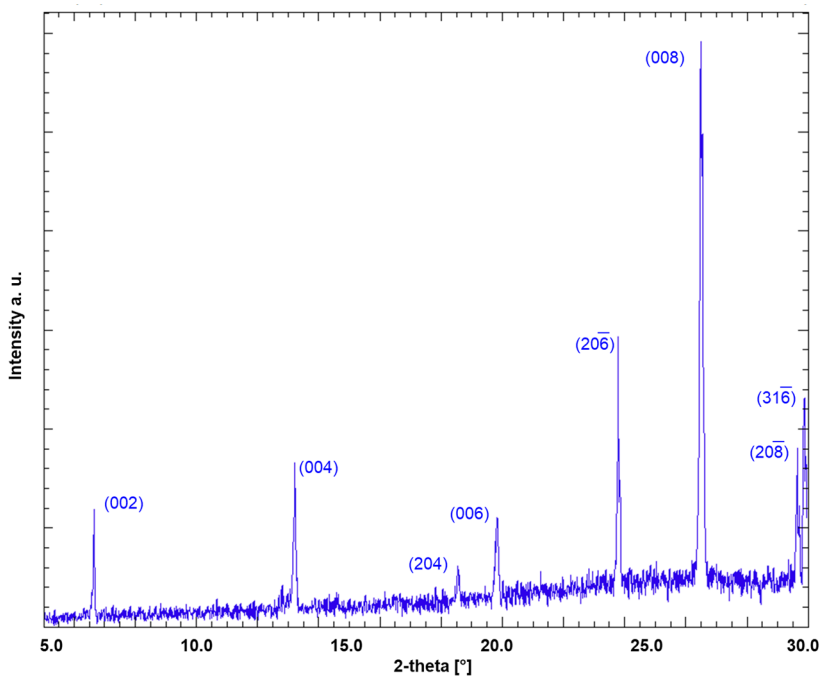

Figure S11. Diffractograms at room temperature after the crystallisation from the melt.

Experiment 2

In experiment 2, the sample was cooled to -170 °C and heated up to 55 °C. Diffraction patterns were collected in 24 different temperature points Changes in the diffraction pattern start occurring at -73 °C where a phase transition occurs between form II and IV. All diffraction patterns in different temperatures can be observed in **Error! Reference source not found.**. After indexing the samples, the variation of the unit cell parameters and refinement fitting for 2-benzoyl-N,N-diethylbenzamide can be observed in Table S5.

Table S5. Variation of the unit cell parameters according to the temperature for the sample BDB.

T (°C)	*T* (K)	*a* (σ_a) / Å	*b* (σ_b) / Å	*c* (σ_c) / Å	β (σ_β) / °	*V* (σ_V) / Å	R_p (%)	R_{wp} (%)	Space Group
-170	103	13.684 (2)	8.4380 (9)	26.766 (2)	90.506 (4)	3090.5 (6)	9.33	12.18	
-163	110	13.696 (2)	8.4423 (10)	26.787 (2)	90.523 (5)	3097.1 (6)	9.68	13.01	
-153	120	13.695 (2)	8.4411 (9)	26.790 (2)	90.507 (5)	3096.7 (5)	9.50	12.61	
-148	125	13.693 (2)	8.4393 (9)	26.788 (2)	90.497 (4)	3095.4 (5)	8.92	11.78	
-143	130	13.697 (1)	8.4414 (8)	26.795 (2)	90.499 (4)	3098.1 (5)	9.06	11.78	
-138	135	13.696 (1)	8.4391 (8)	26.796 (2)	90.488 (4)	3097.0 (5)	8.80	11.59	I 2/a
-133	140	13.700 (1)	8.4415 (8)	26.805 (2)	90.475 (4)	3099.9 (5)	9.06	11.83	
-128	145	13.701 (1)	8.4427 (8)	26.808 (2)	90.476 (4)	3100.9 (5)	8.88	11.66	
-123	150	13.697 (2)	8.4393 (9)	26.804 (2)	90.460 (4)	3098.1 (6)	8.98	11.80	
-118	155	13.708 (2)	8.4423 (9)	26.828 (2)	90.458 (5)	3104.7 (5)	9.24	12.23	
-113	160	13.689 (2)	8.4316 (11)	26.792 (3)	90.442 (4)	3092.2 (7)	9.43	12.21	
-93	180	13.685 (3)	8.4314 (15)	26.820 (4)	90	3094.5 (9)	14.19	19.00	
-73	200	13.695 (2)	8.4314 (13)	26.853 (3)	90	3100.5 (8)	13.04	17.26	
-53	220	13.698 (2)	8.4308 (11)	26.869 (3)	90	3102.9 (7)	11.60	15.31	
-33	240	13.708 (2)	8.4332 (11)	26.896 (3)	90	3109.2 (7)	11.03	14.33	
-13	260	13.707 (2)	8.4310 (10)	26.899 (3)	90	3108.5 (6)	10.66	13.78	
7	280	13.717 (2)	8.4333 (10)	26.924 (2)	90	3114.6 (6)	10.47	13.55	
25	298	13.730 (2)	8.4361 (10)	26.955 (3)	90	3122.1 (6)	10.26	12.98	*I* m m m
27	300	13.737 (2)	8.4390 (10)	26.972 (2)	90	3126.8 (6)	10.06	12.82	
47	320	13.743 (2)	8.4378 (10)	26.993 (2)	90	3130.1 (6)	9.24	11.98	
49	322	13.740 (2)	8.4347 (10)	26.987 (2)	90	3127.6 (6)	9.45	12.17	
51	324	13.747 (2)	8.4379 (9)	26.997 (2)	90	3131.5 (6)	9.54	12.11	
53	326	13.750 (2)	8.4396 (11)	27.008 (2)	90	3134.2 (6)	10.05	12.78	
55	328	13.755 (2)	8.4404 (10)	27.015 (2)	90	3136.4 (6)	10.12	12.99	

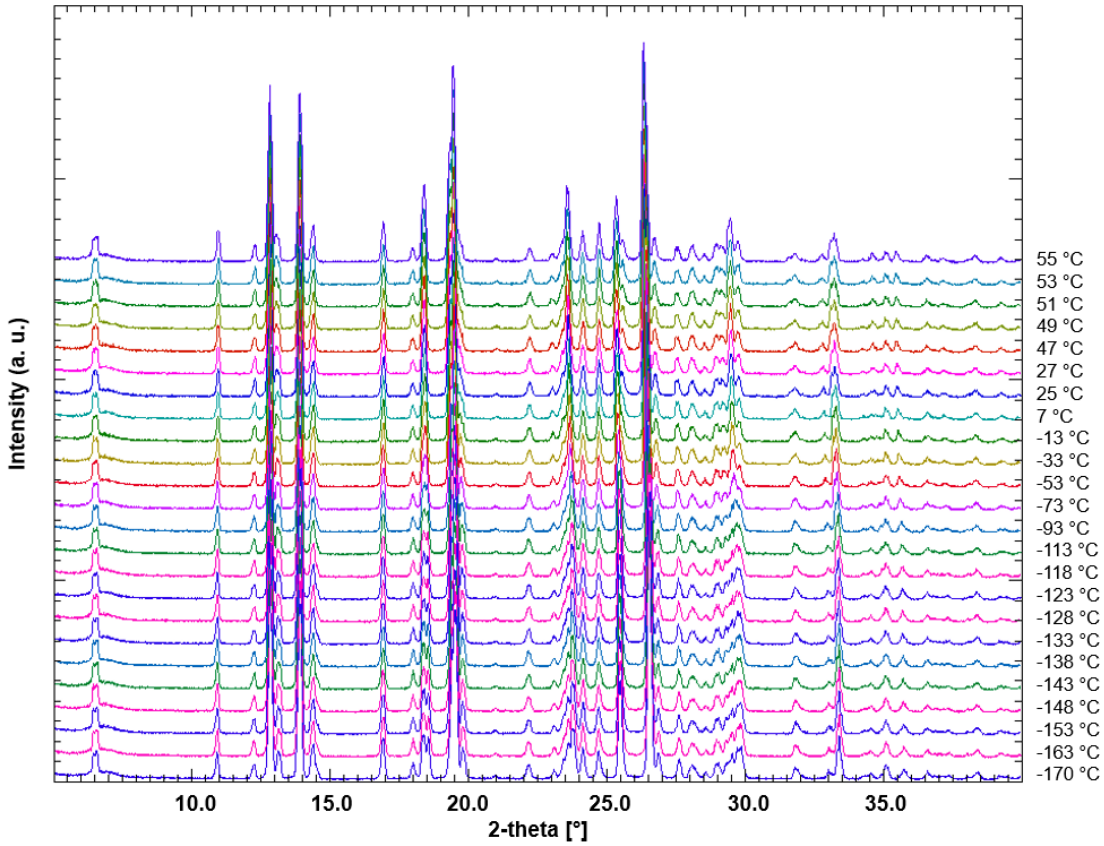

Figure S12. Diffractograms for variable temperature x-ray powder diffraction experiments in 24 different temperature points (T range between -170 °C and 55 °C).

8. References

1. Wei, W.-T. *et al.* Rapid synthesis of isoquinolinones by intramolecular coupling of amides and ketones. *Organic & Biomolecular Chemistry* **13**, 817–824 (2015).
2. Spackman, M. A. & Jayatilaka, D. Hirshfeld surface analysis. *CrystEngComm* **11**, 19–32 (2009).
3. Spackman, M. A. & McKinnon, J. J. Fingerprinting intermolecular interactions in molecular crystals. *CrystEngComm* **4**, 378–392 (2002).
4. Turner, M. J. *et al.* CrystalExplorer17. (2017).
5. Turner, M. J., McKinnon, J. J., Jayatilaka, D. & Spackman, M. A. Visualisation and characterisation of voids in crystalline materials. CrystEngComm 13, 1804–1813 (2011).